# Long-range supercurrents through half-metallic ferromagnetic CrO2

Anwar, M.S.; Czeschka, F.; Hesselberth, M.B.S.; Porcu, M.; Aarts, J.

PHYSICAL REVIEW B **82**, 100501(R) (2010)

# Long-range supercurrents through half-metallic ferromagnetic $CrO_2$

M. S. Anwar,[1,*] F. Czeschka,[2] M. Hesselberth,[1] M. Porcu,[3] and J. Aarts[1,†]
[1]*Kamerlingh Onnes Laboratorium, Leiden University, P.O. Box 9504, 2300 RA Leiden, The Netherlands*
[2]*Walther Meissner Institute, D-85748 Garching, Germany*
[3]*Kavli Institute of Nanoscience, Delft University of Technology, Lorentzweg 1, 2628 CJ Delft, The Netherlands*
(Received 9 August 2010; published 3 September 2010)

We report on measurements of supercurrents through the half-metallic ferromagnet $CrO_2$ grown on hexagonal $Al_2O_3$ (sapphire). The current was observed to flow over a distance of 700 nm between two superconducting amorphous $Mo_{70}Ge_{30}$ electrodes which were deposited on the $CrO_2$ film. The critical current $I_c$ increases as function of decreasing temperature. Upon applying an in-plane magnetic field, $I_c$ goes through a maximum at the rather high field of 80 mT. We believe this to be a long-range proximity effect in the ferromagnet, carried by odd-frequency pairing correlations.

DOI: 10.1103/PhysRevB.82.100501 PACS number(s): 74.45.+c, 72.25.Mk, 74.50.+r, 75.70.Cn

The proximity-effect arising when a ferromagnet (F) is brought into contact with a conventional superconductor (S), is generally assumed to be small. The superconducting pair correlations decay rapidly inside the magnet since the phase coherence between the two spins forming the singlet Cooper pair is broken up by the exchange field $h_{ex}$. In the dirty limit, the decay length $\xi_F \propto 1/\sqrt{h_{ex}}$ is no more than 10 nm even for a weak ferromagnet. To compare, in a normal (N) metal the dephasing is due to temperature fluctuations with a decay length $\xi_N \propto 1/\sqrt{k_B T}$, which can reach microns at low $T$. Long-range proximity (LRP) effects in ferromagnets would be possible with spin-triplet Cooper pairs, since they do not suffer decay through $h_{ex}$, but the orbital $p$ symmetry required by the Pauli principle makes such the pair strongly susceptible to potential scattering by defects in the material. However, under the principle of odd-frequency pairing, also $s$ symmetry is possible,[1,2] and the existence of odd-frequency $s$-wave triplet pairs could lead to LRP effects in dirty ferromagnets. To produce such triplets in the magnet, the singlet Cooper pair on the S side of the interface needs to sample an inhomogeneous magnetization on the F side,[1,2] or in a variant, spin mixing and magnetic disorder at the interface.[3] Fully spin-polarized magnets (also called half-metallic ferromagnet) are particularly interesting since in such materials triplet correlations cannot be broken by spin-flip scattering and the decay length is set by thermal dephasing only.

Subsequently, experimental observations indicating LRP effects were made by Sosnin *et al.*,[4] who found supercurrents flowing in ferromagnetic Ho wires with lengths up to 150 nm using an Andreev interferometer geometry; and by Keizer *et al.*,[5] who found supercurrents induced in half-metallic ferromagnetic $CrO_2$, when superconducting electrodes of NbTiN with separations up to 1 $\mu$m were placed on unstructured films. Even for normal metals this can be considered a very long range. No other experiments were reported for quite some time but this is now rapidly changing. In the last few months, reports came out on Josephson junctions where thin PdNi layers[6] or Ho layers[7] (providing magnetic inhomogeneity) were combined with Co layers and where no decay of the value of the Josephson current was found up to a thickness of 30 nm of the Co layer. Another report came out on superconducting correlations in single crystalline Co nanowires, reaching a distance of a micron.[8]

Neither Ho nor Co is fully spin polarized, and the triplet decay will be set by the spin-diffusion length (order of 100 nm) in both materials. That makes the $CrO_2$ case with its significantly larger decay length of special interest but here the issue of reproducibility has hampered progress. The original report mentioned large variations in the magnitude of the critical (super)current $I_c$ between different samples and many not showing the effect;[5] no other reports on experiments with $CrO_2$ were published. Here we report new observations of supercurrents in $CrO_2$, using devices which are different from the earlier ones in various aspects. We have grown $CrO_2$ films on $Al_2O_3$ (sapphire) rather than on $TiO_2$, which leads to significant differences in film morphology; and the superconducting contacts are made from amorphous (a-)$Mo_{70}Ge_{30}$, rather than from NbTiN. Again we find significant values for $I_c$ even at a separation of about 1 $\mu$m between the electrodes and only small sensitivity to applied magnetic fields up to 0.5 T. Our observations strengthen the conclusion that odd-frequency triplets can generally be induced in ferromagnets, leading to long-range-proximity effects.

A special issue in the device preparation lies in the growth of $CrO_2$ films. Bulk $CrO_2$ is a metastable phase and film growth techniques such as sputtering, pulsed laser deposition, or molecular-beam epitaxy cannot be used. Still, high-quality films can be grown by chemical-vapor deposition at ambient pressure. For this a precursor is used ($CrO_3$), which is heated in a furnace with flowing oxygen that transports the sublimated precursor to a substrate at an elevated temperature, where it decomposes and forms $CrO_2$. The method only works well, however, for substrates with lattice parameters closely matching the $b$ axis of the tetragonal $CrO_2$ ($b$=0.4421 nm), such as $TiO_2$(100) (quasiorthogonal with $b$=0.4447 nm) or $Al_2O_3$(0001) (hexagonal with $a$=0.4754 nm).[9,10] For our experiments, films were grown on both types of substrates in the manner described above, with the precursor at 260 °C, substrates at 390 °C, and an oxygen flow of 100 SCCM (SCCM denotes cubic centimeter per minute at STP). Deposition on $TiO_2$ leads to films with a morphology widely different from films grown on $Al_2O_3$, as can be seen from the images in Fig. 1 made by atomic force microscopy. $TiO_2$ has an almost square surface net and the

 

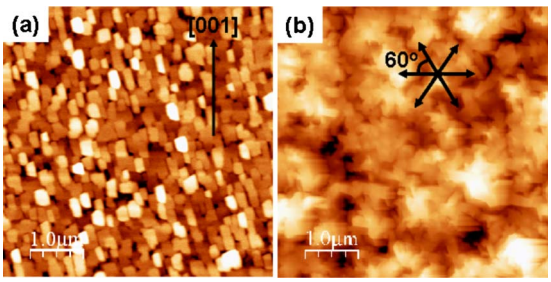


FIG. 1. (Color online) Atomic force microscopy images of $CrO_2$ films grown on (a) a $TiO_2$ substrate; the (001) axis of the substrate is indicated; (b) an $Al_2O_3$ substrate. The different directions of the crystallites which are found in the image are indicated with the arrows and seen to make angles of 60°.

film structure consists of (elongated) platelets as was shown earlier.[11] The hexagonal structure of $Al_2O_3$ leads to growth of crystallites along all six major axes and to considerably more surface roughness. Important is that growth on $Al_2O_3$ does not start as $CrO_2$, but as $Cr_2O_3$, which is isostructural to the sapphire. Only after a layer of about 40 nm has been deposited, the growing film becomes $CrO_2$ as found in Ref. 12. Using transmission electron microscopy (TEM), our finding is similar [Fig. 2(a)]. The $Cr_2O_3$ layer is visible as a dark band of about 30 nm adjacent to the substrate, followed by a brighter area of about 100 nm which is the $CrO_2$ film. The dark band on top is the a-$Mo_{70}Ge_{30}$ used as superconducting contact. Also visible is the columnar structure of the film. Since it is difficult to determine the film thickness from a calibrated deposition time, we used the magnetic properties instead. $Cr_2O_3$ is an antiferromagnetic insulator and $CrO_2$ a ferromagnetic metal with a magnetic moment of 2.0 $\mu_B$/Cr atom ($\mu_B$ is the Bohr magneton), and the measured magnetic moment was used to calculate the $CrO_2$ thickness. The films were characterized by electrical transport measurements. Both specific resistance and saturation magnetization behave as expected, with the (low-temperature) residual resistivity $\rho_0 = 7(10)\mu\Omega$ cm for films on $TiO_2$ ($Al_2O_3$).

The insulating nature of the substrates is an impediment in lithography. In particular, it is difficult to etch a structure into the film and then define electrodes on the bare substrate with electron-beam lithography. Instead, we made the devices by (rf) sputtering 60 nm of (a-)$Mo_{70}Ge_{30}$ electrodes

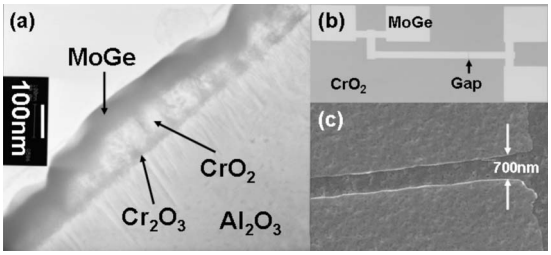


FIG. 2. (a) Transmission electron microscopy image of a $CrO_2$ film grown on $Al_2O_3$. Visible are the substrate, the $Cr_2O_3$ seed layer, the $CrO_2$ layer, and the a-$Mo_{70}Ge_{30}$ layer. (b) Layout of the device structure with four current/voltage contacts. The width of the electrodes is 30 $\mu$m. (c) Scanning electron microscopy image of the gap between the two electrodes, made by liftoff.

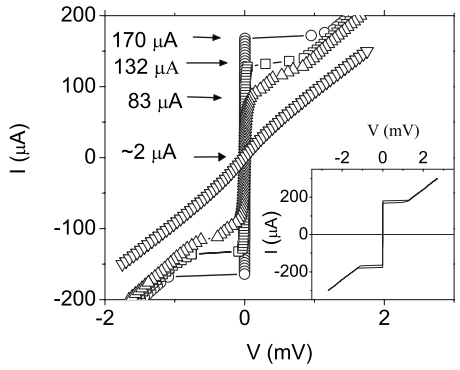


FIG. 3. Current ($I$) versus voltage ($V$) measurements for device A at 2, 3.15, 4, and 6 K. The values of the critical current are indicated. The inset shows an $I$-$V$ characteristic for device B.

with a superconducting transition temperature $T_c \approx 6.5$ K through a lift-off mask onto the unstructured film. Before deposition, the film surface was cleaned briefly with an $O_2$ reactive ion plasma, in order to remove resist or developer residues. Ar-ion etching was applied immediately prior to deposition in order to remove newly formed $Cr_2O_3$ on the film surface. The width of the electrodes was about 30 $\mu$m and the gap between the electrodes around 700 nm. Figures 2(b) and 2(c) show the layout of the electrodes on the film surface and an electron microscopy image of the gap.

A number of devices were prepared in this way and three out of roughly ten showed a supercurrent. We call them A, B, and C; device B was slightly different from the other two in that it consisted of three parallel electrodes rather than one, with a distance between electrodes of 100 $\mu$m and the three gaps measured in parallel. Figure 3 shows the current-voltage ($I$-$V$) characteristic of device A, taken between 6 K (just below $T_c$) and 2.5 K. We observe a clear zero resistance supercurrent branch, with a maximum value for $I_c$ of 170 $\mu$A at 2.5 K. The inset shows data for device B measured at 2 K. From these measurements $I_c$ was determined as the first deviation from the linear $I$-$V$ characteristic around zero bias (equivalent to the peak in the derivative $dI/dV$). The temperature dependence $I_c(T)$ is given in Fig. 4 for all three samples. All devices have very similar values for the critical current, even for the case of three parallel electrodes. The behavior close to $T_c$ is concave rather than linear. In Fig. 5 we present the effect of applying a magnetic field $H_a$ on $I_c$ in device A at a temperature of 3 K. The field was applied in the plane of the film, with a direction either parallel to the long axis of the electrodes (not shown), or perpendicular to that axis. In the first configuration we do not find effects up to 500 mT. In the second configuration we find large changes, however. Starting from zero field, $I_c$ increases by about 10% and goes through a maximum around 80 mT before dropping down to a level which at 500 mT is about 10% below the zero-field value. Sweeping back, the behavior is different, with a relatively sharp jump back to the zero-field level, but no peak as in the forward sweep. Continuing in the negative field quadrant, no structure in $I_c(H_a)$ was found. A point to note is that the maximum lies well outside the hysteresis loop of the magnet. The coercive field $H_c$ is on the order of 10 mT only (inset of Fig. 5). Unfortunately, the

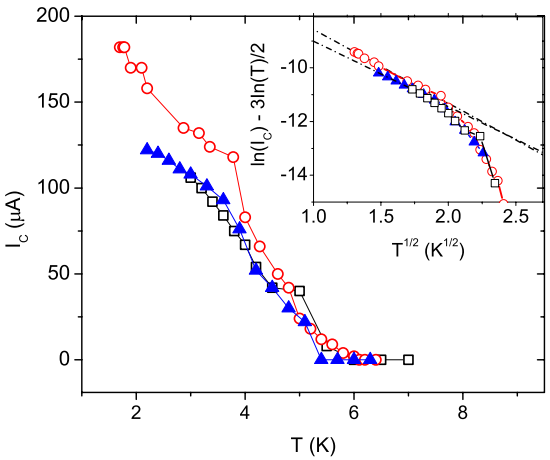


FIG. 4. (Color online) Critical current $I_c$ versus temperature $T$ for devices A (○), B (△), and C (□). The inset shows $\ln I_c - 3/2 \ln T$ versus $T^{1/2}$. Dashed lines correspond to a Thouless energy of 72(91) $\mu$V for device A (B, C).

samples proved fragile and could only be cooled down a few times before the supercurrent disappeared, however, there was no slow degradation when the supercurrent was present.

The results are best discussed in comparison with the previous report on supercurrents in $CrO_2$.[5] First, we can compare their magnitudes by assuming that the current flows homogeneously across the bridge and through the full thickness $d_{CrO_2}$ of the layer. In our case ($d_{CrO_2} \approx 100$ nm, bridge width 30 $\mu$m, current 100 $\mu$A) we find a critical-current density at 2 K of about $3 \times 10^7$ (A/m$^2$). The earlier data ($d_{CrO_2} = 100$ nm, bridge width 2 $\mu$m, typical current 1 mA) correspond to $5 \times 10^9$ (A/m$^2$) and from this point of view there appears to be a large difference between the two results. Comparing the field dependence, in Ref. 5 a Fraunhofer pattern was detected with a distance between maxima of about 90 mT. Assuming this to be equivalent to one flux quantum $\Phi_0$ in the junction area of 310 nm $\times d_{CrO_2}$, a value

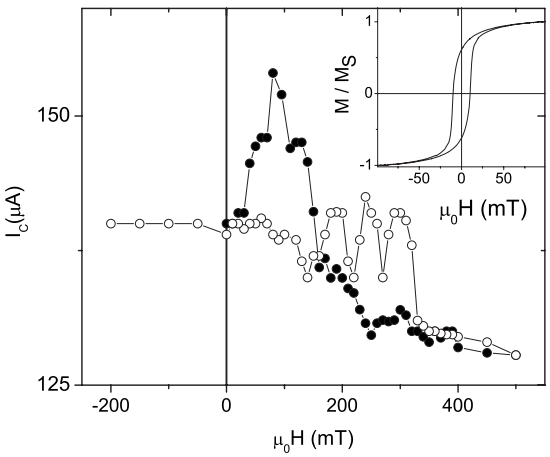


FIG. 5. Dependence of the critical current $I_c$ on a magnetic field in the plane of the junction, perpendicular to the long axis of the electrodes. The inset shows the magnetization $M$ normalized to the saturation magnetization $M_s$ as a function of an in-plane applied field for a $CrO_2$ film grown on sapphire.

of roughly 80 nm is found for $d_{CrO_2}$, quite close to the nominal thickness and suggesting that the full film thickness is partaking in the supercurrent (*casu quo* in the shielding from the magnetic field). In the data set presented here (Fig. 5) a Fraunhofer pattern is not clearly visible but there is a maximum at 80 mT followed by discontinuities around 150 and 250 mT, and a small maximum at 300 mT. Taken together, this suggests a period of 100 mT. For a junction area of 700 nm $\times d_{CrO_2}$, this corresponds to $d_{CrO_2} \approx 30$ nm, which indicates that in our case the current is not flowing through the full thickness of the layer. The picture then emerging is that, although the results are qualitatively the same, the growth on $Al_2O_3$ leads to a somewhat weaker junction. Since the TEM picture in Fig. 2 shows that in our devices grain boundaries will always be in the path of the current, this actually seems a reasonable conclusion. Another point to discuss is that the maximum in the Fraunhofer pattern is not found at zero field, which in Ref. 5 was ascribed to the finite sample magnetization. That is probably not a sufficient explanation since saturation of the magnetization is reached at a significantly smaller field value. However, it has been argued from the magnetoresistance behavior that also intergrain tunneling plays a role,[13] and the intergrain coupling may well still change at higher field than where the magnetization loop has closed.

There is another way to gauge the strength of the junction. According to diffusive theory, $I_c$ for a long S-N-S junction (N a normal metal) is proportional to $T^{3/2} \exp(\sqrt{(2\pi k_B T)/E_{Th}})$, with $E_{Th}$ the Thouless energy given by $(\hbar D)/L^2$, $D$ the diffusion constant of the N metal and $L$ the junction length.[14,15] Plotting $\ln(I_c) - 3/2 \ln(T)$ versus $\sqrt{T}$ (inset of Fig. 4) shows that the relation holds well at low temperatures, with values for $E_{Th}$ of 72(91) $\mu$V for device A (B, C). This in turn can be used to estimate the maximum critical current from the relation $eI_cR_N = 10.8E_{Th}$.[15] The normal resistance $R_N$ of the junction is 11 $\Omega$, which would yield a value for $I_c$ of 75 $\mu$A. This compares well to the measurements but a problem is that the measured $R_N$ is much larger than expected for the $CrO_2$ bridge. Using a typical specific resistance, measured in various films, of 10 $\mu\Omega$ cm, we rather estimate the normal resistance of the junction to be 4 m$\Omega$. This points to a low transparency $\mathcal{T}$ of the S/F barrier, which would correct the prefactor of $E_{Th}$ roughly with $\mathcal{T}$ (Ref. 16) and yield an estimate for $I_cR_N$ lower than the measured value. This issue requires further study.

Overall, the numbers suggest in several ways that the junction critical currents are smaller than what can in principle be obtained. On the other hand, in our working devices the current densities are large enough to conclude that the effect is intrinsic, rather than carried by filamentary normal metal shorts in the ferromagnetic matrix, for which also otherwise no signs exist. Our premise is that the supercurrent is of triplet nature, and a difficulty lies in the preparation of the "spin-active" interface, which should both provide the difference in spin scattering and unaligned magnetic moments.[17] Experimentally, the $CrO_2$ film surface is sensitive to oxidation and has to be cleaned before the superconducting electrodes are deposited. The Ar etching will not only remove unwanted oxides but may also damage the surface in such a

way that the required scattering or magnetization disorder is not present. Especially the fact that device B, which consists of three parallel electrodes rather than one, does not show a larger $I_c$, strongly suggests that the triplet generation takes place at isolated spots under the electrodes rather than homogeneously over their width. Another hindrance is the finite lifetime of the devices, which is probably due to the grainy nature of the films and thermal-expansion differences between film and substrate. These may not be the only bottlenecks, however. One common factor between the earlier experiments using $TiO_2$ and the present ones with sapphire is that the films have more than one easy axis of magnetization. In the case of sapphire, this is due to the strong polycrystalline nature of the growth, particularly evident in Fig. 1(b). In the case of $TiO_2$, it was due to the peculiar circumstance that strain relaxation in the film can lead to a change in the easy-axis direction, with biaxial behavior occurring around a film thickness of 100 nm.[18] Apart from the experiments we report here, we have grown a number of films on $TiO_2$, and we find that growth conditions (including substrate cleaning prior to the growth) crucially determine whether biaxial behavior occurs. The devices we prepared using $TiO_2$ substrates did not show supercurrents but those films showed uniaxial anisotropy at low temperatures so that a true comparison with the earlier work was not made.

In conclusion, we have provided new evidence that a supercurrent can flow through the half-metallic ferromagnet $CrO_2$ over ranges on the order of a micrometer. The odd-frequency pairing scenario appears a plausible one, both from the critical current values and from the magnetic field dependence. However, the analysis shows that the junctions are far from perfect, and that no control as yet exists over the preparation of the spin-active interface. This explains the difficulties in producing reproducible experiments.

We thank T. M. Klapwijk, S. Gönnenwein, H. W. Zandbergen, and V. Ryazanov for useful discussions. M.S.A. acknowledges the financial support of the Higher Education Commission (HEC) Pakistan. This work is part of the research program of the Stichting voor Fundamenteel Onderzoek der Materie (FOM).

*On leave from Dept. of Physics, University of Engineering and Technology, Lahore-54890, Pakistan.

†aarts@physics.leidenuniv.nl

[1] F. S. Bergeret, A. F. Volkov, and K. B. Efetov, Phys. Rev. Lett. **86**, 4096 (2001).

[2] A. Kadigrobov, R. I. Shekhter, and M. Jonson, Europhys. Lett. **54**, 394 (2001).

[3] M. Eschrig and T. Löfwander, Nat. Phys. **4**, 138 (2008).

[4] I. Sosnin, H. Cho, V. T. Petrashov, and A. F. Volkov, Phys. Rev. Lett. **96**, 157002 (2006).

[5] R. S. Keizer, S. T. B. Goennenwein, T. M. Klapwijk, G. Miao, G. Xiao, and A. Gupta, Nature (London) **439**, 825 (2006).

[6] T. S. Khaire, M. A. Khasawneh, W. P. Pratt, Jr., and N. O. Birge, Phys. Rev. Lett. **104**, 137002 (2010).

[7] J. W. A. Robinson, J. D. S. Witt, and M. G. Blamire, Science **329**, 59 (2010).

[8] J. Wang, M. Singh, M. Tian, N. Kumar, B. Liu, C. Shi, J. K. Jain, N. Samarth, T. E. Mallouk and M. H. W. Chan, Nat. Phys. **6**, 389 (2010).

[9] X. W. Li, A. Gupta, T. R. McGuire, P. R. Duncombe, and G. Xiao, J. Appl. Phys. **85**, 5585 (1999).

[10] K. P. Kämper, W. Schmitt, G. Güntherodt, R. J. Gambino, and R. Ruf, Phys. Rev. Lett. **59**, 2788 (1987).

[11] G.-X. Miao, G. Xiao, and A. Gupta, Phys. Status Solidi A **203**, 1513 (2006)

[12] M. Rabe, J. Pommer, K. Samm, B. Özyilmaz, C. König, M. Fraune, U. Rüdiger, G. Güntherodt, S. Senz, and D. Hesse, J. Phys.: Condens. Matter **14**, 7 (2002).

[13] C. König, M. Fonin, M. Laufenberg, A. Biehler, W. Bührer, M. Kläui, U. Rüdiger, and G. Güntherodt, Phys. Rev. B **75**, 144428 (2007).

[14] F. K. Wilhelm, A. D. Zaikin, and G. Schön, J. Low Temp. Phys. **106**, 305 (1997).

[15] P. Dubos, H. Courtois, B. Pannetier, F. K. Wilhelm, A. D. Zaikin, and G. Schön, Phys. Rev. B **63**, 064502 (2001).

[16] A. A. Golubov (private communication).

[17] M. Eschrig, J. Kopu, J. C. Cuevas, and G. Schön, Phys. Rev. Lett. **90**, 137003 (2003).

[18] S. T. B. Goennenwein, R. S. Keizer, S. W. Schink, I. van Dijk, T. M. Klapwijk, G. X. Miao, G. Xiao, and A. Gupta, Appl. Phys. Lett. **90**, 142509 (2007).